ISSN: 2633-4828 Vol. 5 No. S6, (Oct - Dec 2023)

International Journal of Applied Engineering & Technology

PERFORMANCE ENHANCEMENT OF SOLAR AIR HEATERS USING ARTIFICIAL ROUGHNESS: A COMPREHENSIVE REVIEW

Siju Kanji Hamirbhai[1] and Dr. Pravin P. Rathod[2]
[1]Research Scholar, Gujarat Technological University Ahmedabad
[2]Professor, Mechanical Engineering Department, Government Engineering College – Bhuj

Submitted: August 2023 *Revision: September 2023* *Accepted: October 2023*

ABSTRACT
This review examines advancements in the design of solar air heaters (SAHs) by applying artificial roughness to absorber plates. To address the inherent limitations in heat transfer and thermo-hydraulic performance associated with conventional SAHs, various roughness geometries have been introduced. A wide range of experimental and analytical investigations has demonstrated that artificial roughness significantly improves thermal efficiency by increasing the Nusselt number and friction factor across broad Reynolds number ranges. The paper compiles these strategies, emphasizing the influence of artificial roughness modifications on overall system performance.

Keywords: *Solar Air Heater, Artificial Roughness, Heat Transfer, Nusselt Number, Pressure Drop*

NOMENCLATURE

A	surface area of absorber plate (m^2)
D	equivalent or hydraulic diameter of duct (m)
e	rib height (m)
g	groove position (m)
h	heat transfer coefficient (W/m^2K)
H	height of duct (m)
I	intensity of solar radiation (W/m^2)
L	length of test section (m)
m	mass flow rate (kg/s)
p	pitch (m)
P	Pressure drop (Pa)
S	length of discrete rib or short way length of mesh (m)
w	width of rib (m)
W	width of duct (m)
Dimensionless parameters	
B/S	relative roughness length
d/w	relative gap position
e/D	relative roughness height
f	friction factor

g/e	relative gap width
L/e	relative long way length of mesh
l/s	relative length of metal grit
Nu	Nusselt number
Nu_s	Nusselt number for smooth channel
Nu_r	Nusselt number for rough channel
p/e	relative roughness pitch
Pr	Prandlt number
Re	Reynolds number
St	Stanton number
S/e	relative short way length of mesh
W/H	duct aspect ratio

1. INTRODUCTION

Solar energy is the fundamental origin of nearly all energy forms on Earth. Fossil fuels such as coal, oil, and natural gas, as well as biomass, are derivatives of ancient photosynthetic activity followed by geological transformations. Even wind and tidal energies are driven by solar-induced atmospheric and lunar effects. Historically, solar energy has been harnessed for practical purposes such as drying agricultural products, with the distinct advantage of being clean and environmentally sustainable.

Solar radiation that directly strikes the Earth's surface without being diffused by atmospheric particles is known as **beam radiation**, which typically constitutes around 80% to 85% of the total incoming solar energy. The remaining 15% to 20% is classified as **diffuse radiation**, which results from scattering due to clouds and atmospheric molecules. Additionally, a fraction of the incident radiation is reflected back into the atmosphere, further contributing to the overall energy distribution dynamics on the Earth's surface [27].

Despite the vast quantity of solar radiation reaching the Earth’s surface, it is not feasible to capture all of it due to atmospheric losses and technological limitations. Therefore, it is essential to develop advanced methods and technologies that can efficiently harness and convert as much solar energy as possible to meet growing energy demands. Solar energy can be captured using either **passive** or **active** methods. Passive methods involve the indirect conversion of solar radiation into usable forms—such as through architectural design for natural lighting or heating—without the use of mechanical devices. In contrast, active methods utilize mechanical or electrical systems to directly convert solar radiation into useful energy forms, such as thermal or electrical energy.

Among the various technologies developed to utilize solar energy, **solar air heaters (SAHs)** are recognized for their structural simplicity, low cost, and minimal maintenance requirements. Their primary applications include space heating, timber seasoning, industrial product curing, and drying of construction materials like clay and concrete blocks [1]. A typical SAH comprises a flat absorber plate and an insulating base, creating a duct through which air flows and absorbs thermal energy from the sun.

The core components of a typical solar air heater include a **transparent glass cover**, **absorber plate**, **insulated casing or frame**, and **air inlet and outlet ducts**. The frame—usually made of wood or metal—supports the structural assembly. The absorber plate, positioned beneath the glass cover, captures incident solar radiation and converts it into heat, which is then transferred to the air flowing through a duct beneath the plate. **Thermal insulation** surrounds the bottom and sides of the collector to minimize heat losses. Figure 1 illustrates the basic construction of a conventional flat plate air heater.

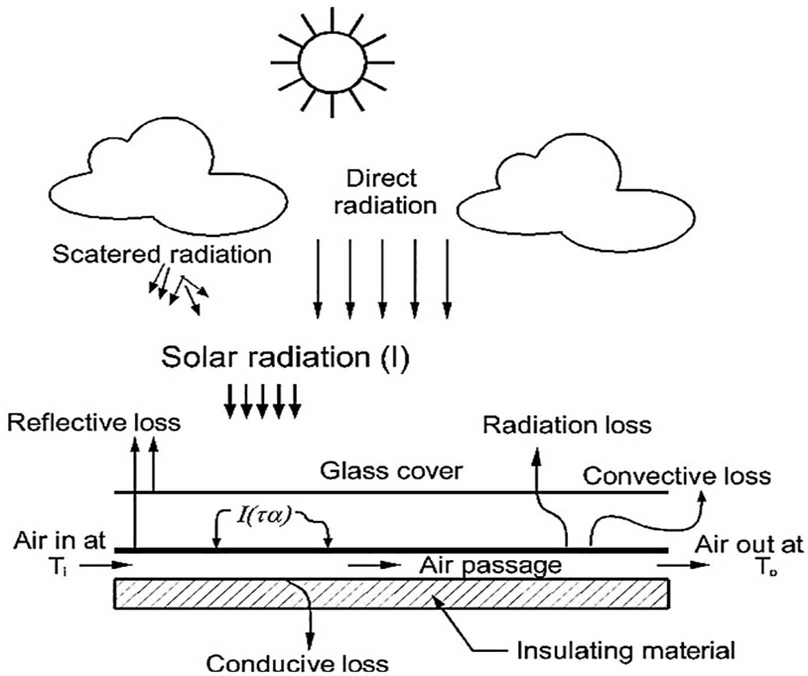

Fig. 1. Conventional Solar air heating device [29].

Solar air heaters can be classified based on the **method of energy extraction** and their **intended application**. According to the classification presented by Tyagi VV et al [28], these devices are categorized to suit diverse operational needs and functional configurations, as outlined in Figure 2.

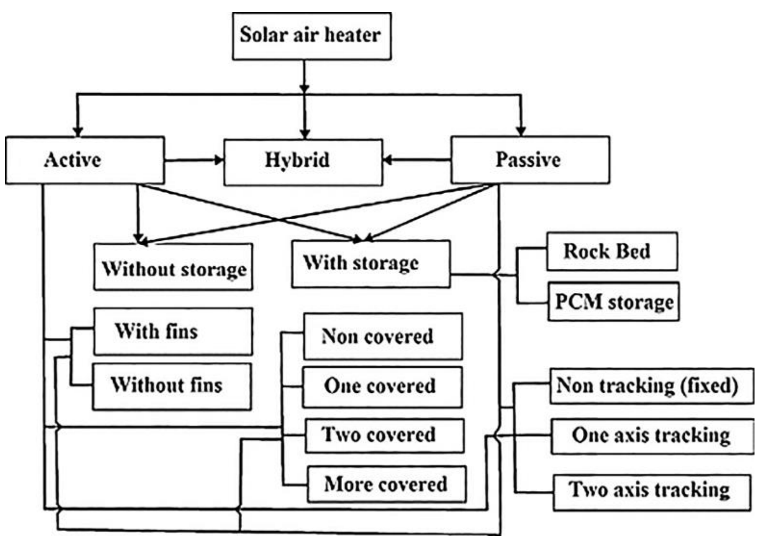

Fig. 2. Classification of the solar air heating technology [28].

Solar air heaters (SAHs) find extensive application across various domains including **heating, ventilation, and air conditioning (HVAC)** systems, **greenhouse season extension**, **textile drying**, and **marine product treatment**. A particularly common use is in **agricultural crop drying**, where air temperatures in the range of 45–70 °C are often required—readily achievable using solar air heaters [30]. During colder seasons, air heated through SAHs can be utilized via **natural or forced convection** methods for **space heating**, offering a sustainable alternative to conventional HVAC systems, especially in areas with limited access to electrical energy.

However, a major limitation in solar air heaters arises due to the formation of a **laminar viscous sub-layer** adjacent to the absorber plate. This layer restricts convective energy transfer between the heated surface and the passing air, resulting in a **low convective heat transfer coefficient** and consequently reduced system efficiency.

This has motivated widespread research into **heat transfer augmentation techniques**, particularly the use of **artificial roughness elements** introduced on the underside of the absorber plate. These elements disrupt the laminar sub-layer and promote turbulence, thereby improving heat transfer. However, an inherent trade-off exists—**increased turbulence also leads to higher pressure drop**, which negatively impacts the system's hydraulic performance. Therefore, **a comprehensive evaluation of both thermal and hydraulic performance** is critical in the design of efficient solar air heaters.

To enable comparative assessment of different SAH configurations, researchers such as Webb & Eckert [31] and Lewis [32] introduced performance evaluation parameters like the **Thermo-Hydraulic Enhancement Factor (THEF)** and the **Thermo-Hydraulic Performance Parameter (THPP)**. These are defined as follows:

$$\text{Thermo-Hydraulic Enhancement Factor (THEF)} = \frac{Nu_r/Nu_s}{\left(f_r/f_s\right)^{\frac{1}{3}}} \quad (1)$$

$$\text{Thermo-Hydraulic Performance Parameter (THPP)} = \frac{St_r/St_s}{\left(f_r/f_s\right)^{\frac{1}{3}}} \quad (2)$$

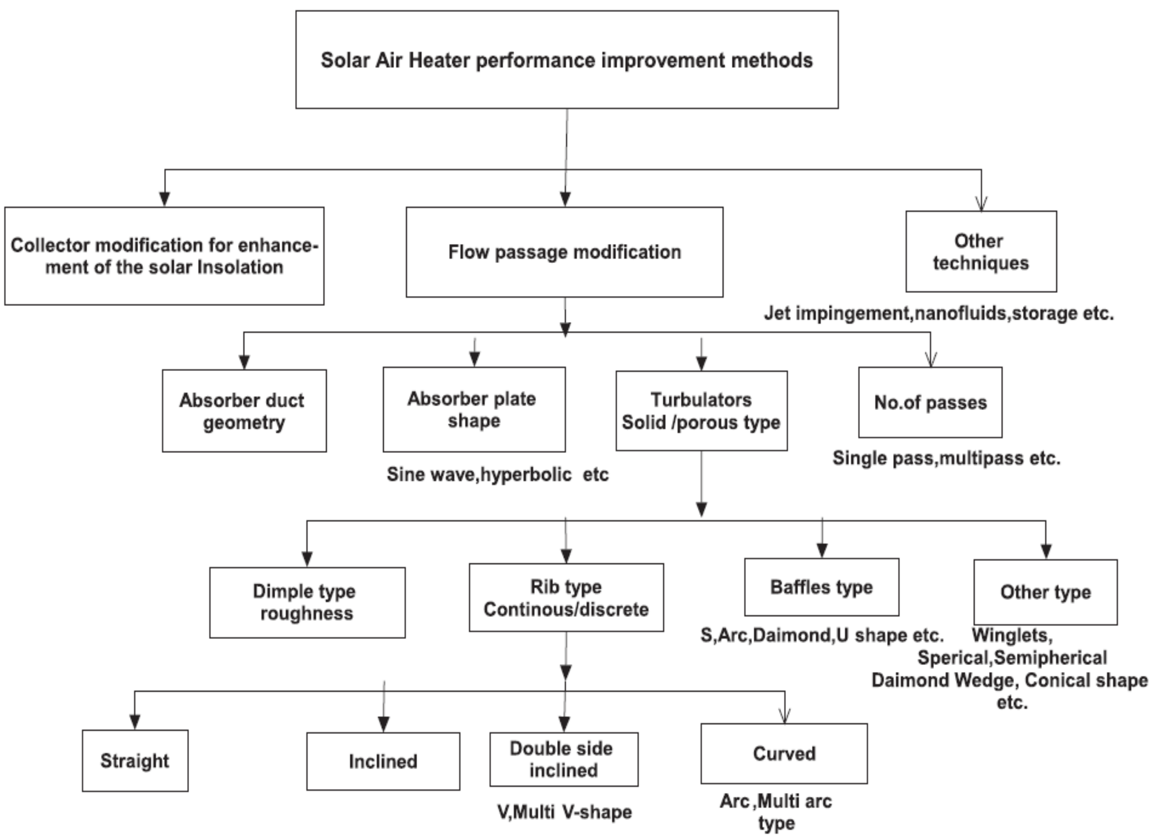

Fig. 3. Physical representation of the performance improvement methods in the solar air heater [33].

Extensive research efforts have been devoted to optimizing the design of solar air heaters (SAHs) in order to improve their overall performance. These studies emphasize the need for design modifications that can enhance both thermal efficiency and fluid dynamic behaviour, with minimal penalties in pressure drop.

A significant focus has been placed on modifying the **flow passage area**, particularly the absorber duct region, as it plays a central role in determining the thermal and thermo-hydraulic characteristics of the system. These modifications are generally categorized into the following major types:

(a) Turbulators Attached to the Absorber Plate: These elements are introduced to induce turbulence within the duct, disrupting the boundary layer and promoting convective heat transfer.

(b) Absorber Plate Modifications: Altering the physical texture or structure of the absorber plate enhances airflow characteristics and surface heat exchange.

(c) Geometric Modifications of the Duct: Adjusting the overall shape or cross-sectional geometry of the absorber duct influences flow distribution and heat transfer behaviour.

(d) Multi-Flow Path Designs: Employing multiple or redirected airflow paths increases the interaction between air and the heated surface, further improving energy capture.

Each of these strategies aims to strike a balance between maximizing heat transfer and minimizing flow resistance.

Effect of a Rib

Artificial roughness introduced on the underside of the absorber plate plays a critical role in altering the flow dynamics within a solar air heater duct. Specifically, when ribs are employed as roughness elements, they create **flow separation zones** on either side of the rib structure. The separated flow leads to the generation of **vortices**, which induce turbulence in the near-wall region. This increased turbulence enhances convective heat transfer by disrupting the thermal boundary layer. However, this benefit is accompanied by a rise in **frictional losses**, as the turbulent motion increases the pressure drop across the duct. The influence of rib height on the stability and thickness of the laminar sub-layer is illustrated in Figure 4 [34].

Effect of Rib Height and Pitch

The spacing and size of the rib elements—quantified as **rib height** and **rib pitch**—have a direct impact on the downstream flow patterns and thermal performance. Figures 5 and 6 illustrate how variations in these parameters affect flow reattachment behaviour [35]. After flow separates at the leading edge of a rib, it may reattach further downstream, forming a re-circulating zone. Notably, when the **relative roughness pitch (p/e)** is less than 8, the flow does not reattach effectively, limiting the enhancement in heat transfer.

Maximum heat transfer typically occurs near the reattachment point, where turbulence is most intense. Enhanced thermal performance can be achieved either by **reducing the relative roughness pitch (p/e)** for a given rib height or by **increasing the relative roughness height (e/D)** for a fixed pitch. However, experimental findings suggest that when the relative roughness pitch exceeds a value of 10, the heat transfer enhancement begins to decline. This implies that there is an optimal range of rib geometry where heat transfer is maximized without excessively increasing flow resistance.

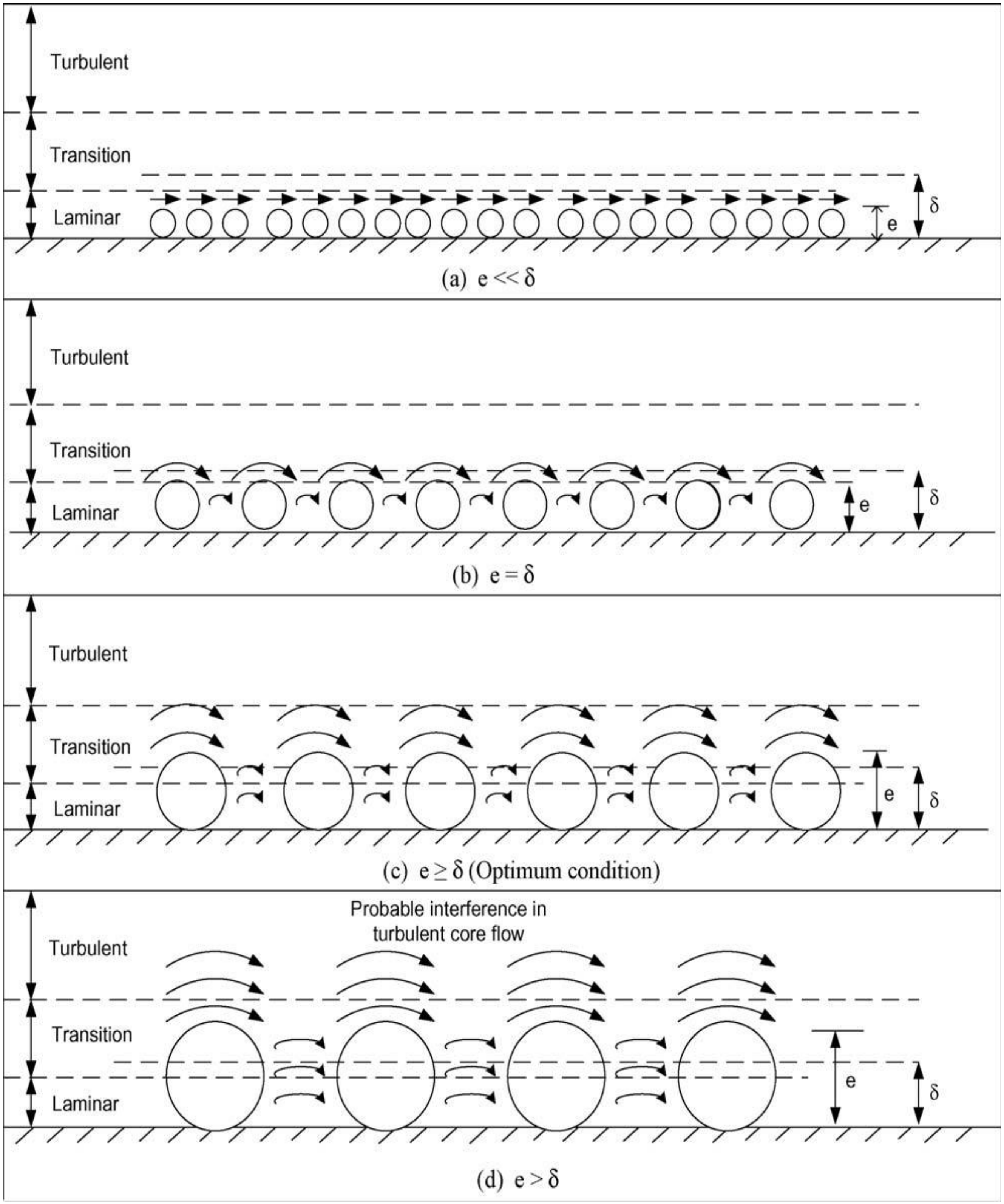

Fig. 4. Effect of rib height on laminar sub layer [34].

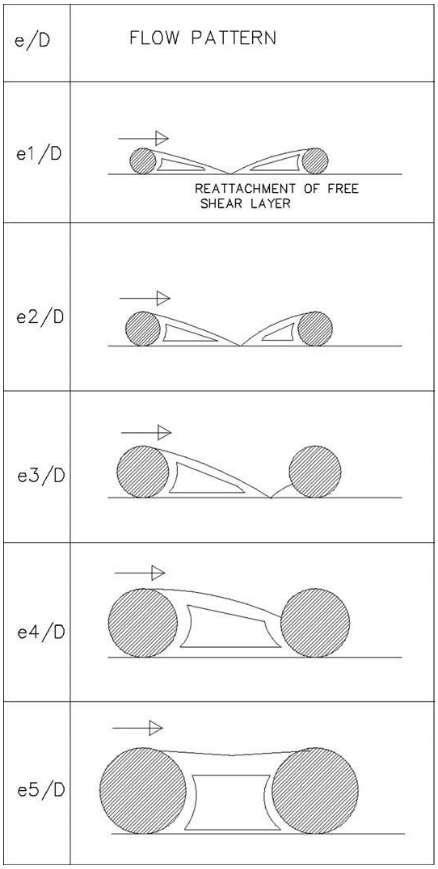

Fig. 5. Effect of rib roughness height on flow pattern (e5 > e4 > e3 > e2 > e1, p = constant) [35].

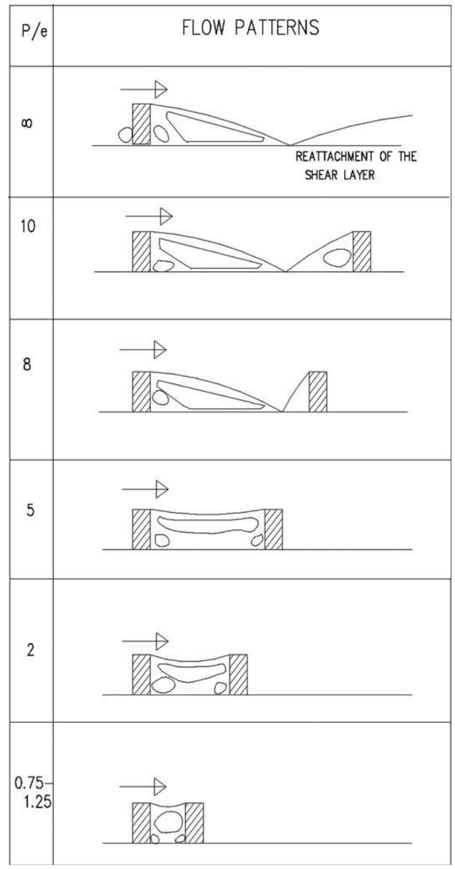

Fig. 6. Flow pattern of rib as a function of relative roughness pitch [35].

2. Artificial Roughness Geometries

Artificial roughness significantly improves the thermal and hydraulic performance of solar air heaters by disrupting the laminar sub-layer and enhancing turbulence. Various geometries—such as transverse, inclined, V-shaped, and broken ribs etc. have been shown to promote mixing and increase heat transfer rates.

2.1 Transverse Wire Rib Roughness

The application of artificial roughness in solar air heaters (SAHs) was pioneered by Prasad and Mullick [2], who introduced small-diameter wires affixed to the underside of the absorber plate to improve thermal performance, particularly for drying applications (Figure 7). Their findings indicated that these protruding wires increased the plate efficiency factor from 0.63 to 0.72, translating into a 14% enhancement in thermal performance at a Reynolds number of 40,000. Furthermore, the experimentally measured heat transfer coefficients exhibited good agreement with theoretical predictions, validating the effectiveness of this approach.

Verma and Prasad [3] conducted an outdoor experimental study to optimize the thermohydraulic performance of SAHs using transverse wire roughness. Their investigation encompassed a Reynolds number (Re) range of 5,000 to 20,000, a relative roughness pitch (P/e) of 10 to 40, and a relative roughness height (e/D) of 0.01 to 0.03. The study involved three rectangular duct configurations two roughened and one smooth and evaluated the effect of wire ribs affixed to the underside of the absorber plate (Figure 7). The optimal value of the roughness Reynolds number (e^+) was identified as 24, at which point the thermo-hydraulic performance peaked at 71%. The heat transfer enhancement factor (Nu_r/Nu_s) varied between 1.25 and 2.08 within the investigated parameter range. Additionally, empirical correlations were formulated for both Nusselt number and friction factor.

Further insights were provided by Prasad [4], who examined the thermal behaviour of SAHs with transverse wire roughness under fully developed turbulent flow conditions in real outdoor environments. In this study, thin galvanized iron (G.I.) wires of various diameters were positioned perpendicularly to the airflow on the absorber plate. The results showed significantly enhanced thermal performance when compared to smooth duct collectors. Specifically, the ratios of heat removal factor, collector efficiency factor, and overall thermal efficiency for roughened collectors compared to their smooth counterparts were 1.786, 1.806, and 1.842, respectively, over the examined operational range.

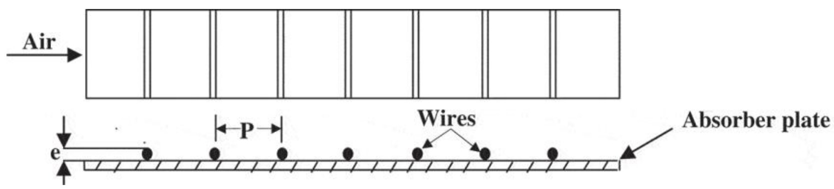

Fig. 7. Transverse wire rib roughness

2.2 90° Broken Transverse Rib Roughness

Sahu and Bhagoria [5] conducted an experimental investigation into the influence of 90° broken transverse ribs (Figure 8) on the thermal performance of solar air heaters. The study employed a fixed roughness height (e) of 1.5 mm, corresponding to a relative roughness height (e/D) of 0.0338, and utilized a duct with an aspect ratio (W/H) of 8. The pitch (P) of the ribs was varied within the range of 10 to 30 mm, while the Reynolds number (Re) was examined across a spectrum of 3,000 to 12,000.

Results demonstrated that the Nusselt number achieved its peak at a roughness pitch of 20 mm, after which further increases in pitch led to a decline in thermal performance. The use of broken ribs significantly enhanced the heat transfer coefficient by approximately 1.25 to 1.4 times when compared with a smooth duct operating under similar conditions, particularly at higher Reynolds numbers. The experimental data further indicated that the thermal efficiency of the roughened solar air heater varied between 51% and 83.5%, contingent upon the specific flow conditions. These findings underscore the effectiveness of broken rib geometries in augmenting heat transfer without excessively increasing flow resistance.

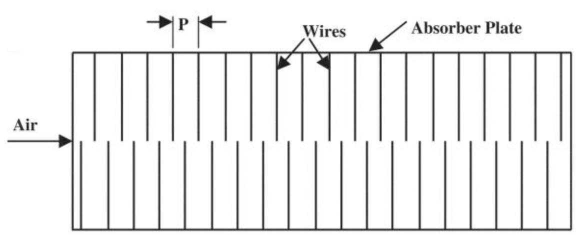

Fig. 8. 90° broken transverse rib roughness

2.3 Inclined Wire Rib Roughness

Gupta, Solanki, and Saini [6] conducted a detailed experimental study to assess the impact of inclined transverse wire rib roughness on the thermal and fluid dynamic characteristics of solar air heaters. The experiments were performed within the transitionally rough flow regime, specifically in the range of $5 < e^+ < 70$. The test setup included rectangular solar air heater ducts with absorber plates featuring inclined wire ribs installed on the underside (Figure 9).

Through this investigation, the authors developed empirical correlations for both the Nusselt number and the friction factor. These correlations were expressed as functions of the rib geometry, duct cross-sectional area, and the Reynolds number (Re) of the airflow. A key finding was that inclined ribs (i.e., non-transverse orientations) offered superior performance compared to standard transverse ribs, particularly in enhancing the heat transfer coefficient.

The results indicated that the highest improvements in thermal and frictional performance occurred at inclination angles of 60° and 70°, yielding enhancements in heat transfer and friction factor by factors of approximately 1.8 and 2.7, respectively. Optimal thermo-hydraulic efficiency was observed at a relative roughness height (e/D) of 0.023 and a Reynolds number of 14,000. These findings affirm the benefits of angular rib configurations in achieving more effective thermal performance in solar air heater systems.

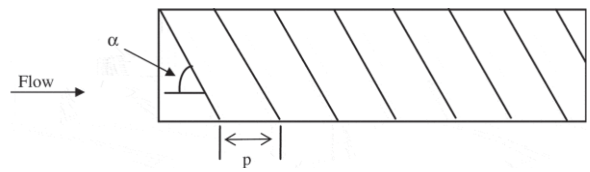

Fig. 9. Inclined wire rib roughness

2.4 Inclined Continuous Ribs Roughness with Gap

Aharwal, Gandhi, and Saini [7] experimentally examined the heat transfer and friction behavior of solar air heater ducts equipped with integral, repeated discrete square ribs on the absorber plate (Figure 10). The study focused on the influence of key geometrical parameters specifically, the width and position of the gaps introduced between the ribs.

Compared to a smooth absorber surface, the rib-roughened configuration demonstrated significant performance gains. The Nusselt number and friction factor increased by approximately 2.83 and 3.60 times, respectively, over the investigated parameter range. The most notable enhancement in heat transfer was achieved at a relative gap position of 0.25 and a relative gap width of 1.0. These conditions were paired with a relative roughness pitch of 8, an angle of attack of 60°, and a relative roughness height of 0.037.

Additionally, the study found that the maximum friction factor occurred with discrete transverse ribs at a relative roughness pitch of 8. Empirical correlations for both the Nusselt number and the friction factor were derived as functions of the roughness geometry and flow Reynolds number, offering predictive insights for optimizing ribbed absorber plate designs in SAH systems.

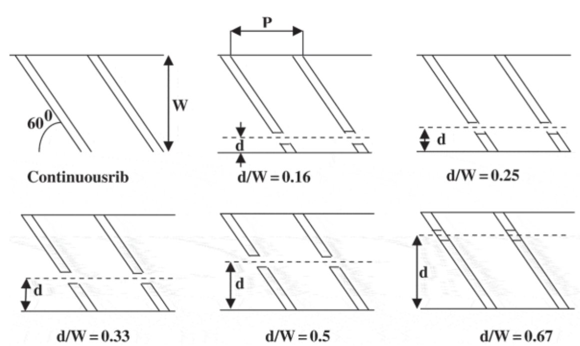

Fig. 10. Inclined continuous ribs roughness with gap

2.5 Combination of Transverse and Inclined Rib Roughness

Varun, Saini, and Singal [8] conducted an experimental study to evaluate the thermal and frictional behaviour of solar air heaters incorporating a hybrid configuration of transverse and inclined ribs on the absorber plate (Figure 11). Their investigation revealed that a relative roughness pitch (p/e) of 8 yielded the highest thermal performance among the tested configurations. Based on the experimental data, the authors developed correlations for the Nusselt number and friction factor that account for the combined rib geometry and flow conditions.

Further extending this line of research, Mittal and Varun [9] experimentally assessed the thermo-hydraulic performance of solar air heaters featuring similar hybrid roughness configurations. Their results indicated that among three rib geometries tested, the configuration with transverse and inclined ribs at a relative pitch (P/e) of 8 demonstrated the best overall performance. It was consistently observed that the thermo-hydraulic efficiency of the roughened solar air heater exceeded that of the smooth duct across the entire range of Reynolds numbers investigated.

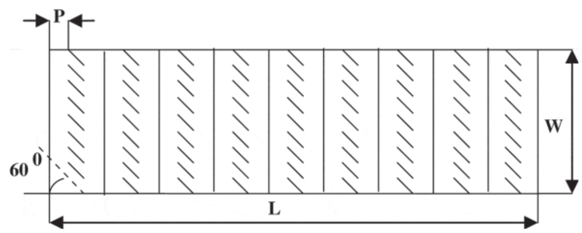

Fig. 11. Combination of transverse and inclined rib roughness

2.6 Expanded Metal Mesh Roughness

Saini and Saini [10] conducted an experimental study to examine the influence of expanded metal mesh as artificial roughness on the thermal and hydraulic performance of solar air heaters. The investigation was performed under fully developed turbulent flow conditions in a rectangular duct with a high aspect ratio of 11:1. The absorber plate was roughened using an expanded metal mesh, as illustrated in Figure 12.

The study revealed a significant enhancement in heat transfer, reporting a maximum improvement of approximately four times that of a smooth duct. This enhancement corresponded to an angle of attack of 61.9°, a relative longway mesh length of 46.87, and a relative shortway length of 25. In contrast, the peak friction factor was observed at an angle of attack of 72°, with a relative longway length of 71.87 and a shortway length of 15.

To support design applications, the authors developed empirical correlations for both the Nusselt number and friction factor based on the geometrical parameters of the expanded metal mesh and the flow Reynolds number. These results underscore the potential of metal mesh roughness to significantly improve heat transfer in SAH systems, albeit with increased flow resistance.

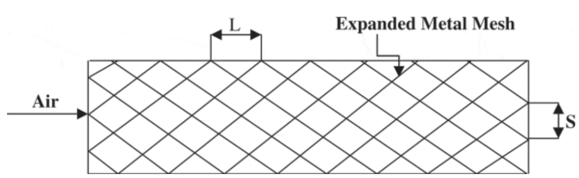

Fig. 12. Expanded metal mesh roughness

2.7 Metal Grit Rib Roughness

Karmare and Tikekar [11] carried out an experimental analysis to evaluate the thermal and hydraulic performance of rectangular solar air heater ducts roughened with metal grit ribs. The ducts used had an aspect ratio of 10:1, and the grit ribs were applied to the absorber surface as shown in Figure 13. The results demonstrated that the use of metal grit ribs could enhance the Nusselt number by up to two times and the friction factor by up to three times compared to a smooth duct, across the range of parameters investigated.

The configuration that yielded the highest heat transfer performance featured roughness parameters of l/s=1.72, e/D=0.044, and P/e=17.5. Interestingly, while this setup maximized thermal performance, a different configuration with P/e=12.5 recorded the highest friction factor under the same l/s and e/D values. The study established that optimal performance was achieved with the roughness geometry of l/s=1.72, e/D=0.044, and P/e=17.5. Correlations for the Nusselt number and friction factor were developed based on the experimental findings.

In a subsequent study, Karmare and Tikekar [12] further examined the thermo-hydraulic performance of solar air heaters employing metal rib grit roughness. Their findings indicated a significant improvement in thermal efficiency—ranging from 10% to 35%—in comparison to heaters with smooth absorber plates. However, this enhancement came with a marked increase in pumping power requirements, due to the associated rise in the friction factor, which was reported to increase by 80% to 250%. These results highlight a performance trade-off between heat transfer improvement and pressure drop penalty in grit rib applications.

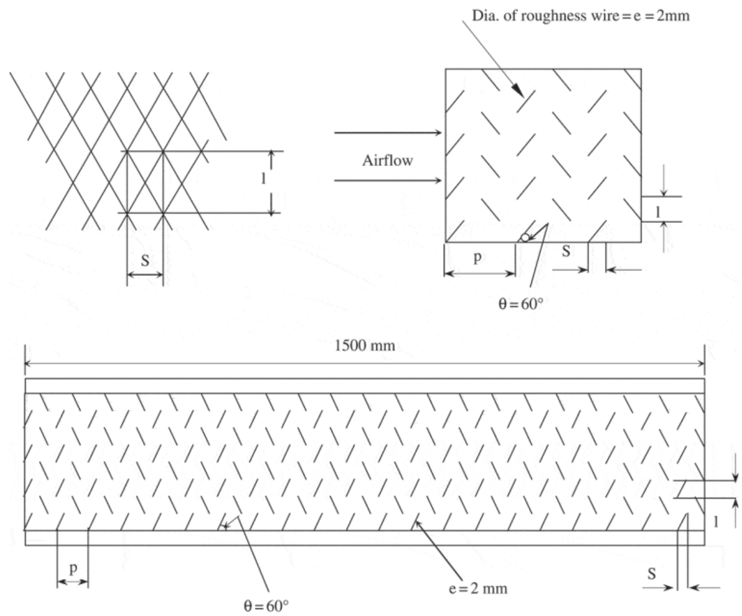

Fig. 13 Metal grit rib roughness

2.8 V-Shaped Rib Roughness

Momin, Saini, and Solanki [13] conducted an experimental investigation to evaluate the influence of V-shaped rib geometries on the heat transfer and fluid flow characteristics in rectangular ducts of solar air heaters (Figure 14). Their study focused on how variations in geometrical parameters particularly the angle of attack and relative roughness height impact thermal and hydraulic performance.

Several key conclusions emerged from the research. First, the implementation of V-shaped ribs led to a substantial increase in performance, with the Nusselt number and friction factor enhanced by factors of 2.30 and 2.83, respectively, compared to a smooth duct. These peak enhancements were observed at an angle of attack of 60°, which was identified as the optimal inclination for maximizing both heat transfer and frictional resistance.

Second, the thermo-hydraulic performance parameter was shown to improve with increases in both the angle of attack and the relative roughness height, with performance maxima consistently occurring at a 60° angle. Third, when comparing configurations, the V-shaped ribs demonstrated superior performance over both inclined ribs and smooth absorber plates. At a relative roughness height of 0.034 and Reynolds number of 17,034, the enhancement in Nusselt number was found to be 1.14 times that of inclined ribs and 2.30 times that of a smooth surface.

The authors also developed empirical correlations for predicting the Nusselt number and friction factor based on the rib geometry and flow parameters, providing a useful tool for optimizing the design of SAHs employing V-shaped roughness elements.

Fig. 14. V-shaped rib roughness

2.9 Staggered Discrete V-Shaped Rib Roughness

Muluwork [14] conducted a comparative analysis of staggered discrete V-shaped ribs—with apex orientations facing upward and downward—against their transverse staggered discrete counterparts, to assess their thermal performance in solar air heaters (Figure 15). The study focused on evaluating the influence of multiple roughness parameters, including the relative roughness length ratio (B/S), relative roughness segment ratio (S′/S), relative roughness staggering ratio (p′/p), and angle of attack (α), on both the heat transfer rate and the friction factor.

The findings indicated that the Nusselt number consistently increased with higher values of the relative roughness length ratio (B/S), highlighting its positive influence on thermal enhancement. Among the tested configurations, the V-down discrete ribs outperformed both V-up and transverse rib geometries in terms of heat transfer augmentation. Furthermore, increasing the relative roughness staggering ratio (p′/p) led to improved thermal performance, reaching a peak at a staggering ratio of 0.6.

The study also reported that both the Nusselt number and friction factor achieved their maximum values at angles of attack of 60° and 70°, respectively. Based on the experimental results, empirical correlations for predicting the Nusselt number and friction factor were developed as functions of the aforementioned roughness and flow parameters. These outcomes highlight the strong potential of staggered discrete V-down ribs for improving the efficiency of SAH systems through enhanced turbulence and mixing.

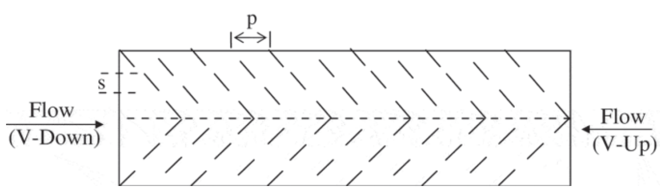

Fig. 15. Staggered discrete V-shaped rib roughness

2.10 Multi V-Shaped Rib Roughness

Hans, Saini, and Saini [15] conducted an experimental study to evaluate the effect of multiple V-shaped rib roughness on the heat transfer coefficient and friction factor in a solar air heater (Figure 16). The investigation aimed to assess how various geometrical parameters of the rib configuration influenced the thermo-hydraulic performance under turbulent flow conditions. Empirical correlations were developed for the Nusselt number and friction factor as functions of roughness geometry and flow parameters.

The results revealed that the use of multiple V-ribs led to significant performance enhancements. The Nusselt number and friction factor were found to be up to 6 and 5 times greater, respectively, than those observed in smooth duct configurations. The maximum heat transfer enhancement occurred at a relative roughness width (W/w) of 6, whereas the friction factor peaked at a relative roughness width of 10.

Additionally, both thermal and hydraulic performance metrics reached their highest values at an angle of attack (α) of 60°. Similarly, the optimum relative roughness pitch (P/e) for both Nusselt number and friction factor was identified as 8. The study also found a monotonic increase in both parameters with increasing relative roughness height (e/D), reinforcing the effectiveness of multi V-shaped ribs in disrupting the boundary layer and promoting turbulent mixing. These findings emphasize the utility of multi-ribbed configurations for maximizing the heat transfer potential in artificially roughened SAHs.

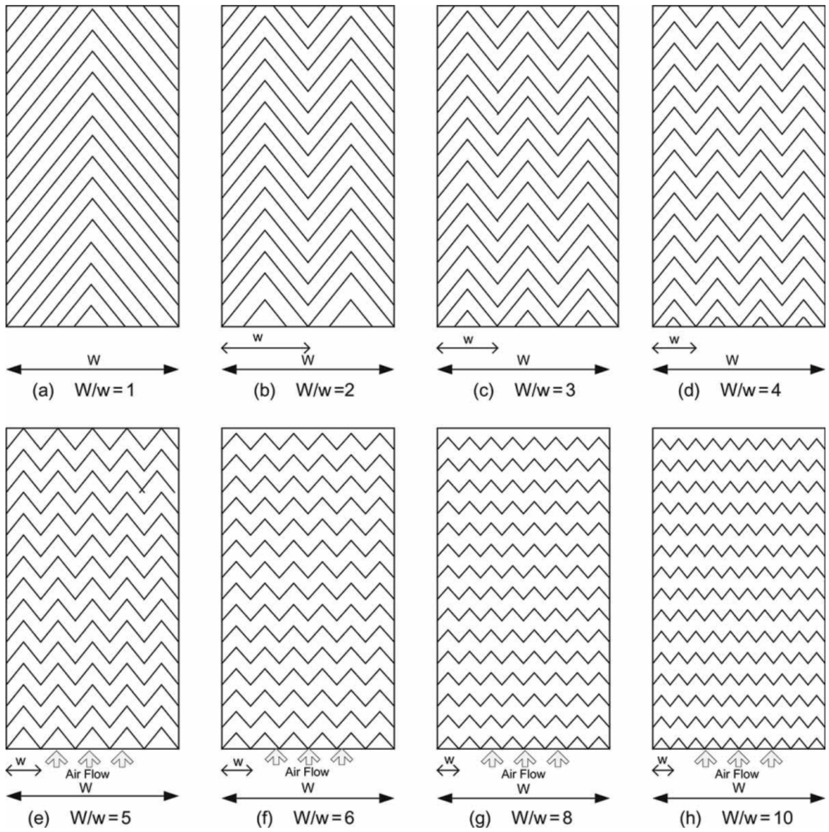

Fig. 16. Multi V-shaped rib roughness

2.11 Discrete V-Down Rib Roughness

Singh, Chander, and Saini [16] experimentally analyzed the heat transfer and fluid flow characteristics of a rectangular duct solar air heater featuring discrete V-down ribs applied to one heated broad wall (Figure 17). The results demonstrated substantial performance improvements when compared to a smooth duct. Specifically, the Nusselt number and friction factor were enhanced by factors of 3.04 and 3.11, respectively, over the range of parameters investigated.

Optimal thermal and frictional performance was observed at a relative roughness pitch (P/e) of 8.0, with both values declining when the pitch deviated from this optimum. A similar pattern was reported for the angle of attack (α), relative gap position (d/w), and relative gap width (g/e). The Nusselt number and friction factor reached their peak values at an angle of attack of 60°, a relative gap position of 0.65, and a relative gap width of 1.0. The authors also developed statistical correlations for both performance metrics, expressing them in terms of Reynolds number and rib geometry parameters.

Complementing these findings, Karwa and Chitoshiya [17] investigated the thermo-hydraulic performance of a solar air heater employing 60° V-down discrete rib roughness on the airflow side of the absorber plate. Compared to a smooth duct, thermal efficiency improvements ranged from 12.5% to 20%, with the highest gains occurring at lower airflow rates. The study also presented a detailed mathematical model to predict the performance behavior and analyzed how variations in design parameters influence the overall thermo-hydraulic response of the system.

These investigations collectively demonstrate the efficacy of discrete V-down rib roughness in improving SAH performance, particularly when optimally configured for pitch, angle, and spacing.

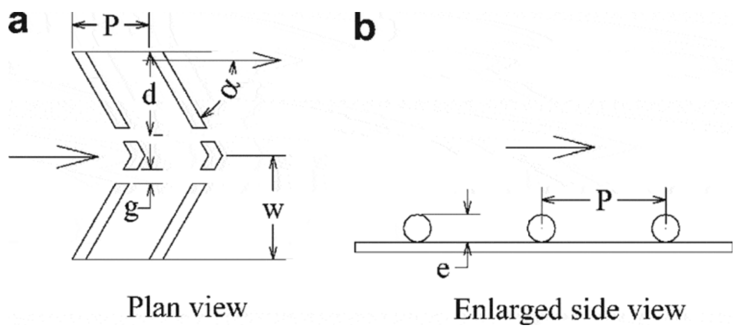

Fig. 17. Discrete V-down rib roughness

2.12 Multi V-Shaped Rib Roughness with Gap

Kumar, Saini, and Saini [18] experimentally investigated the influence of geometrical parameters of multi V-shaped ribs with intermittent gaps on the heat transfer and fluid flow characteristics of a rectangular duct (Figure 18). The ribs were affixed to the underside of the heated absorber plate. Their results revealed substantial enhancements in thermal and hydraulic performance. Specifically, the Nusselt number and friction factor increased by factors of 6.32 and 6.12, respectively, compared to a smooth duct.

The study identified that optimal thermo-hydraulic performance occurred at a relative gap distance of 0.69 and a relative gap width of 1.0. These gap parameters were found to play a pivotal role in breaking the boundary layer and promoting secondary flows, thereby maximizing heat transfer efficiency while maintaining a manageable pressure drop.

In a subsequent investigation, Kumar, Saini, and Saini [19] extended their analysis by examining airflow in ducts with multi V-shaped ribs with gaps installed on one broad wall. This study further confirmed the performance benefits of this configuration. The Nusselt number was found to increase by as much as 6.74 times, and the friction factor by up to 6.37 times compared to a smooth duct, across the range of parameters examined. The highest friction factor was observed for ribs with a relative roughness width of 10.

Both studies developed empirical correlations for the Nusselt number and friction factor based on the rib geometry and Reynolds number. These findings underscore the potential of gapped multi V-shaped rib structures to significantly boost heat transfer performance while enabling careful control of flow resistance in solar air heater ducts.

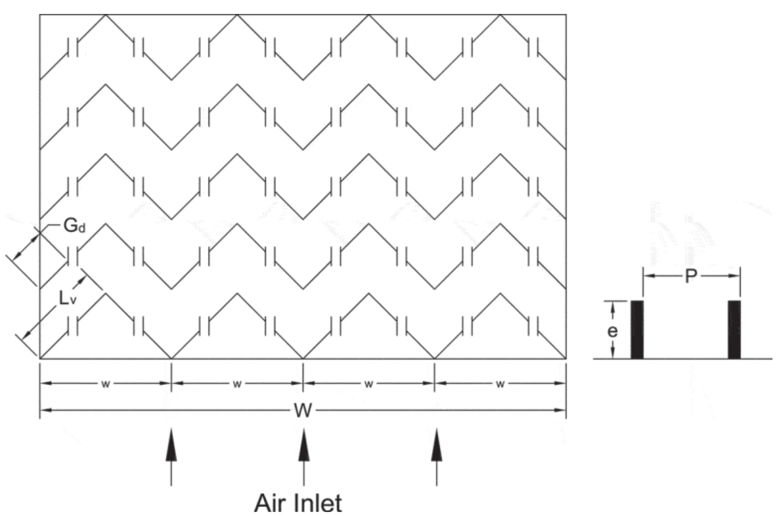

Fig. 18. Multi V-shaped rib roughness with gap

2.13 Arc Shaped Rib Roughness

Saini and Saini [20] conducted an experimental investigation to examine the impact of arc-shaped ribs on the thermal and fluid flow performance of rectangular ducts used in solar air heaters (Figure 19). The study aimed to evaluate how the curvature of the rib influences heat transfer enhancement and flow resistance.

The results demonstrated that the maximum improvement in the Nusselt number—up to 3.80 times compared to a smooth duct—was achieved at a relative arc angle (α/90) of 0.3333 and a relative roughness height of 0.0422. Notably, this enhancement in heat transfer was accompanied by a relatively modest increase in friction factor, recorded at just 1.75 times that of the smooth duct under the same conditions.

These findings suggest that arc-shaped ribs offer a favorable balance between thermal performance and hydraulic losses. Based on the experimental observations, the authors developed empirical correlations for both the Nusselt number and friction factor as functions of the relevant geometrical and flow parameters. This rib configuration presents a promising approach for improving the efficiency of solar air heaters with controlled pressure drop penalties.

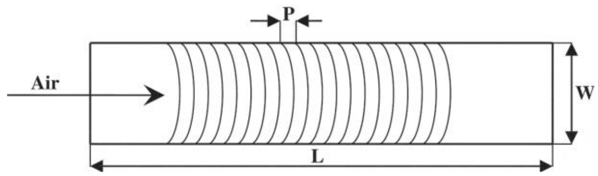

Fig. 19. Arc shaped rib roughness

2.14 Dimple Shaped Rib Roughness

Saini and Verma [21] conducted an experimental study to investigate the fluid flow and heat transfer characteristics of solar air heater ducts equipped with dimple-shaped artificial roughness elements (Figure 20). The focus of the study was to understand the influence of dimple geometry on thermal performance and frictional behavior.

The findings revealed that the maximum Nusselt number occurred at a relative roughness height (e/D) of 0.0379 and a relative roughness pitch (P/e) of 10. This configuration produced the most favorable heat transfer enhancement among the tested setups. Conversely, the lowest friction factor was achieved at a slightly smaller relative roughness height of 0.0289, also at a pitch ratio of P/e = 10, indicating a configuration with minimal hydraulic penalty.

The study underscores the potential of dimple-shaped roughness elements to significantly enhance thermal performance while maintaining acceptable frictional losses. Empirical correlations for the Nusselt number and friction factor were developed from the collected experimental data, providing valuable tools for predicting system behavior under various flow and geometric conditions.

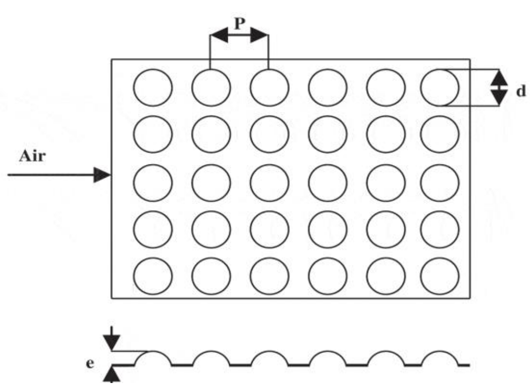

Fig. 20. Dimple shaped rib roughness

2.15 Dimple-Shaped Roughness Arranged in Angular Arc Shape

Sethi, Varun, and Thakur [22] investigated the heat transfer and friction factor characteristics of solar air heater ducts featuring dimple-shaped roughness elements arranged in an angular arc configuration on the absorber plate (Figure 21). Their experimental study focused on understanding how the angular positioning of dimples influences thermohydraulic performance. The maximum Nusselt number was achieved for a relative roughness height of 0.036, a relative roughness pitch of 10, and an arc angle of 60°. From the observed results, statistical correlations were formulated to express the Nusselt number and friction factor as functions of Reynolds number and geometric roughness parameters.

In a related study, Yadav et al. [23] explored the thermal and hydraulic behavior of turbulent airflow through a rectangular duct roughened with circular protrusions also arranged in an angular arc formation (Figure 21). The test setup included a uniformly heated roughened wall, while the remaining three walls were insulated. Their results indicated a maximum heat transfer enhancement of 2.89 times and a friction factor increase of 2.93 times relative to a smooth duct. These peak values were observed at a relative roughness height (e/D) of 0.03, a relative roughness pitch (P/e) of 12, and an arc angle (α) of 60°.

The authors developed empirical correlations to predict the Nusselt number and friction factor based on these parameters. The findings collectively emphasize the effectiveness of angular arc configurations in promoting turbulence and improving the thermo-hydraulic performance of solar air heaters.

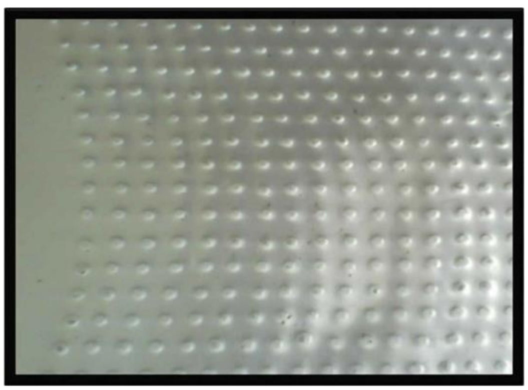

Fig. 21. Dimple shaped roughness arranged in angular arc shape

2.16 W-Shaped Rib Roughness

Lanjewar, Bhagoria, and Sarviya [24] performed an experimental analysis to study the heat transfer and friction factor characteristics of a rectangular duct roughened with W-shaped ribs. These ribs were arranged at an angle relative to the airflow direction and mounted on the underside of one broad wall of the duct (Figure 22). The study evaluated two rib orientations—W-down (pointing downstream) and W-up (pointing upstream).

The results showed a notable increase in thermal performance due to the artificial roughness. For W-down ribs at an angle of attack of 60°, the Nusselt number improved by 136% over a smooth duct, while W-up ribs at the same angle yielded a 124% enhancement. In terms of flow resistance, the friction factor increased by 101% for W-down ribs and by 135% for W-up ribs under the same flow conditions. The maximum thermo-hydraulic performance parameter was observed to be 1.98 for W-down ribs and 1.81 for W-up ribs, indicating that the downstream orientation provided a better overall efficiency. Based on the data collected, correlations for the Nusselt number and friction factor were developed to facilitate predictive analysis.

In a separate study, Lanjewar, Bhagoria, and Sarviya [25] further explored the thermal and hydraulic behavior of ducts roughened with W-shaped ribs oriented at an angle to the flow direction (Figure 22). This investigation confirmed the effectiveness of this rib configuration, reporting maximum enhancements in the Nusselt number and friction factor of 2.36 and 2.01 times, respectively, compared to a smooth duct—both occurring at an angle of attack of 60°. The optimum thermo-hydraulic performance was also achieved at this angle. Correlations for both the heat transfer coefficient and friction factor were derived to assist in the design of efficient roughened SAH systems.

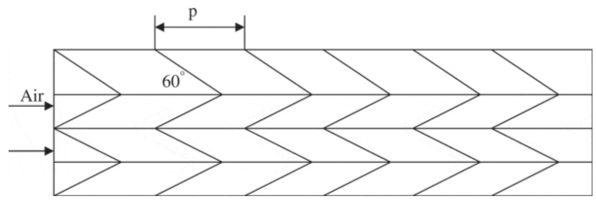

Fig. 22. W-shaped rib roughness

2.17 Discrete W-Shaped Rib Roughness

Kumar, Bhagoria, and Sarviya [26] conducted an experimental study to analyze the thermal and hydraulic performance of a solar air heater roughened with discrete W-shaped ribs (Figure 23). The ribs were installed on one broad wall of a rectangular duct with an aspect ratio of 8:1 to investigate their effect on heat transfer enhancement and flow resistance.

The study reported a significant improvement in performance due to the introduction of discrete W-shaped roughness. The Nusselt number was enhanced by a factor of 2.16, while the friction factor increased by 2.75 times in comparison to a smooth duct. These peak values were obtained at an angle of attack of 60° and a relative roughness height of 0.0338, confirming the effectiveness of this rib orientation for generating turbulence and enhancing heat transfer.

Based on the observed data, the authors developed empirical correlations for the Nusselt number and friction factor as functions of both roughness geometry and flow Reynolds number. These findings highlight the potential of discrete W-shaped rib configurations to significantly boost thermal efficiency while maintaining a practical balance with pressure losses in solar air heater systems.

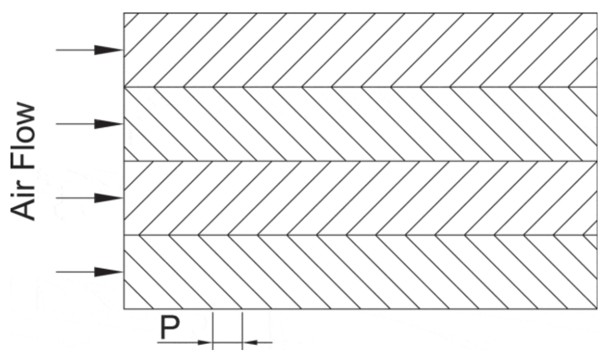

Fig. 23. Discrete W-shaped rib roughness

2.18 S Shaped ribs with gap

Dengjia Wanga et al [36] found that artificial roughness of S shaped ribs with gap (Figure 24) significantly improves solar air heater performance, achieving a maximum thermal efficiency of 65% at a 30 mm channel height. The highest enhancements in Nusselt number (5.42) and friction factor (5.87) occurred at Re = 19,258, W/w = 4, p/e = 20, and g/e = 1.5. Efficiency increased with air mass flow rate, while smaller rib spacing and width further enhanced performance. A 30% gain in efficiency was observed when reducing duct height from 50 mm to 30 mm, though pressure drop also increased. Air passage height had the most significant impact on efficiency.

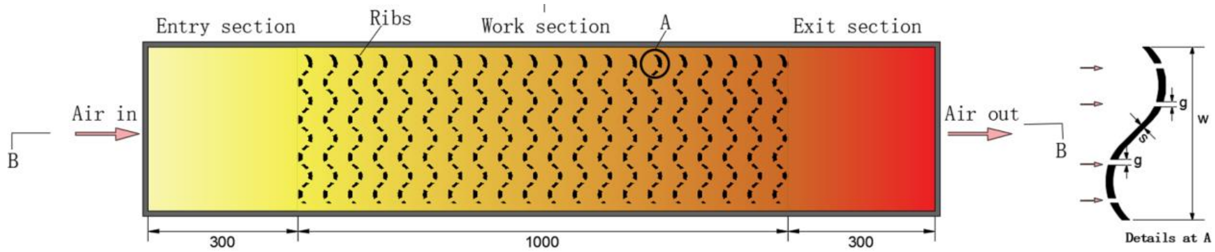

Fig. 24. S Shaped ribs with gap

3. Results and Discussion

The thermo-hydraulic performance of solar air heaters (SAHs) is greatly influenced by the geometry and arrangement of artificial roughness elements. From the compiled data, it is evident that rib shapes significantly affect both heat transfer and pressure drop characteristics. Among conventional rib geometries, circular ribs achieved the highest THPP of 2.3, followed by rectangular–semi-circular (2.1) and hyperbolic ribs (2.18). Advanced rib designs such as multi arc ribs with staggered gaps and multi V-shaped ribs with gaps exhibited outstanding performance, reaching THPP values of 3.6 and 3.7, respectively, due to enhanced turbulence generation and reattachment zones.

Hybrid configurations like continuous ribs with staggered gap (SG) or semi-rotating mixed grooves (SRMG) also performed notably well, with THPP values above 3.0, indicating a significant improvement over simpler geometries. In contrast, traditional shapes such as triangular, square-wave, and truncated ribs showed lower THPPs, ranging from 1.3 to 1.44, reflecting their limited contribution to sustained turbulence.

The results also highlight that downstream-chamfered and reverse L-shaped ribs perform comparably to semi-circular and square ribs (THPP ≈ 1.9–1.95), suggesting optimized flow reattachment with moderate friction loss. Overall, ribs incorporating secondary flow mechanisms or staggered flow paths were more efficient in balancing heat transfer enhancement with hydraulic penalty. This clearly demonstrates that geometric customization of rib structures is vital for maximizing SAH performance.

Table 1: Thermo-hydraulic Performance Parameter of various Rib Geometry

Sr. No.	Rib-geometry	THPP
1	Rectangular Transverse rib	1.89
2	Square Transverse rib	1.94
3	Triangular Transverse rib	1.44
4	Circular Transverse rib	2.3
5	Semi-circular Transverse rib	1.95
6	Downstream-chamfered Transverse rib	1.95
7	Wedged Transverse rib	1.91
8	Chamfered-rib-grooved Transverse rib	1.76
9	Rectangular-rib-grooved Transverse rib	1.79
10	Reverse L-shape Transverse rib	1.9
11	Rectangular – Semicircular Transverse rib	2.1
12	Hyperbolic Transverse rib	2.18
13	Truncated Transverse rib	1.3
14	Square-wave Transverse rib	1.43

15	Continuous Inclined Rib	1.8
16	Continuous inclined with staggered rib	1.8
17	Continuous V Shape ribs	1.9
18	Continuous V shape with staggered ribs	2.06
19	W-down rib	2
20	Multi staggered V-ribs	3.7
21	Continuous Arc-shape rib	1.7
22	Continuous staggered Arc-shape rib	2.37
23	Multi arc rib	3.4
24	Multi staggered arc rib	3.6
25	S-shape rib	3.34

4. CONCLUSION

This review confirms that artificial roughness significantly improves the thermo-hydraulic efficiency of solar air heaters, with performance highly dependent on rib geometry and configuration. Enhanced rib designs such as multi V and multi arc shapes with staggered gaps achieved the highest THPPs, indicating superior heat transfer with acceptable pressure loss. While simpler geometries offer moderate gains, optimized and hybrid structures provide significant enhancement potential. The study underscores the importance of geometry-driven turbulence optimization and offers a direction for designing efficient and cost-effective SAHs for low- to medium-temperature solar applications.

REFERENCES

[1] Yadav, A. S., and J. L. Bhagoria. 2013. Renewable energy sources- an application guide. *International Journal of Energy Science* 3 (2): 70 90.

[2] Prasad K., and S.C. Mullick. 1983. Heat transfer characteristics of a solar air heater used for drying purposes. *Applied Energy* 13 (2): 83-93.

[3] Verma, S.K., and B.N. Prasad. 2000. Investigation for the optimal thermohydraulic performance of artificially roughened solar air heaters. *Renewable Energy* 20 (1): 19-36.

[4] Prasad, B. N. 2013. Thermal performance of artificially roughened solar air heaters. Solar Energy 91: 59-67.

[5] Sahu, M.M., and J.L. Bhagoria. 2005. Augmentation of heat transfer coefficient by using 90^{o} broken transverse ribs on absorber plate of solar air heater. *Renewable Energy* 30 (13): 2057- 2073.

[6] Gupta, D., S.C. Solanki, and J.S. Saini. 1993. Heat and fluid flow in rectangular solar air heater ducts having transverse rib roughness on absorber plates. *Solar Energy* 51 (1): 31-37.

[7] Aharwal, K.R., B.K. Gandhi, and J.S. Saini. 2009. Heat transfer and friction characteristics of solar air heater ducts having integral inclined discrete ribs on absorber plate. *International Journal of Heat and Mass Transfer* 52 (25-26): 5970-5977.

[8] Varun, R.P. Saini, and S.K. Singal. 2008. Investigation of thermal performance of solar air heater having roughness elements as a combination of inclined and transverse ribs on absorber plate. *Renewable Energy* 33 (6): 1398-1405.

[9] Mittal, M.K., and Varun. 2009. Thermohydraulic performance of solar air heater provided with artificial roughness on the absorber plate. *Institute of Engineers Journal IE (I)–MC* 92 (July): 43- 48.

[10] Saini, R.P., and J.S. Saini. 1997. Heat transfer and friction factor correlations for artificially roughened ducts with expanded metal mesh as roughened element. *International Journal of Heat and Mass Transfer* 40 (4): 973-986.

[11] Karmare, S.V., and A.N. Tikekar. 2007. Heat transfer and friction factor correlation for artificially roughened duct with metal grit ribs. *International Journal of Heat and Mass Transfer* 50 (21-22): 4342–4351.

[12] Karmare, S.V., and A.N. Tikekar. 2009. Experimental investigation of optimum thermohydraulic performance of solar air heaters with metal rib grits roughness. *Solar energy* 83 (1): 6-13.

[13] Momin, A.M.E., J.S. Saini, and S.C. Solanki. 2002. Heat Transfer and Friction in Solar Air Heater Duct with V-Shaped Rib Roughness on Absorber Plate. *International Journal of Heat and Mass Transfer* 45 (16): 3383-3396.

[14] Anil Singh Yadav & Manish Kumar Thapak, 2015, Artificially Roughened Solar air Heater: A Comparative Study, International Journal of Green Energy, volume 13, Issue 2.

[15] Hans, V.S., R.P. Saini, and J.S. Saini. 2010. Heat transfer and friction factor correlations for a solar air heater duct roughened artificially with multiple v-ribs. *Solar Energy* 84 (6): 898-991.

[16] Singh, S., S. Chander, and J.S. Saini. 2011. Heat transfer and friction factor correlations of solar air heater ducts artificially roughened with discrete v-down ribs. *Energy* 36 (8): 5053-5064.

[17] Karwa, R., and G. Chitoshiya. 2013. Performance study of solar air heater having v-down discrete ribs on absorber plate. *Energy* 55: 939-955.

[18] Kumar, A., R.P. Saini, and J.S. Saini. 2012. Experimental investigation on heat transfer and fluid flow characteristics of air flow in a rectangular duct with multi v shaped rib with gap roughness on the heated plate. *Solar Energy* 86 (6): 1733-1749.

[19] Kumar, A., R.P. Saini, and J.S. Saini. 2013. Development of correlations for Nusselt number and friction factor for solar air heater with roughened duct having multi v-shaped with gap rib as artificial roughness. *Renewable Energy* 58: 151-163.

[20] Saini, S.K., and R.P. Saini. 2008. Development of correlations for nusselt number and friction factor for solar air heater with roughened duct having arc shaped wire as artificial roughness. *Solar Energy* 82 (12): 1118-1130.

[21] Saini, R.P., and J. Verma. 2008. Heat transfer and friction factor correlations for a duct having dimple-shaped artificial roughness for solar air heaters. *Energy* 33 (8): 1277-1287.

[22] Sethi, M., Varun, and N.S. Thakur. 2012. Correlations for solar air heater duct with dimpled shape roughness elements on absorber plate. *Solar Energy* 86 (9): 2852 2861.

[23] Yadav, S., M. Kaushal, Varun, and Siddhartha. 2013. Nusselt number and friction factor correlations for solar air heater duct having protrusions as roughness elements on absorber plate. *Experimental Thermal and Fluid Science* 44: 34-41.

[24] Lanjewar, A., J.L. Bhagoria, and R.M. Sarviya. 2011. Experimental study of augmented heat transfer and friction in solar air heater with different orientations of w-rib roughness. *Experimental Thermal and Fluid Science* 35 (6): 986-995.

[25] Lanjewar, A., J.L. Bhagoria, and R.M. Sarviya. 2011b. Heat transfer and friction in solar air heater duct with w-shaped rib roughness on absorber plate. *Renewable Energy* 36 (7): 4531-4541.

[26] Kumar, A., J.L. Bhagoria, and R.M. Sarviya. 2009. Heat transfer and friction correlations for artificially roughened solar air heater duct with discrete w-shaped ribs. *Energy Conversion and Management* 50 (8): 2106–2117.

[27] Tian Y, Zhao CY. A review of solar collectors and thermal energy storage in solar thermal applications. Appl Energy 2013; 104:538–53.

[28] Tyagi VV, Panwar NL, Rahim NA, Kothari R. Review on solar air heating system with and without thermal energy storage system. Renew Sustain Energy Rev 2012;16(4):2289–303.

[29] Yadav AS, Thapak MK. Artificially roughened solar air heater: experimental investigations. Renew Sustain Energy Rev 2014; 36:370–411.

[30] Tchinda R. A review of the mathematical models for predicting solar air heaters systems. Renew Sustain Energy Rev 2009;13(8):1734–59.

[31] Webb RL, Eckert ERG, Goldstein RJ. Heat transfer and friction in tubes with repeated- rib roughness. Int J Heat Mass Transf 1971;14(4):601–17.

[32] Lewis MJ. Optimising the thermohydraulic performance of rough surfaces. Int J Heat Mass Transf 1975;18(11):1243–8.

[33] H.S. Arunkumar, K. Vasudeva Karanth, Shiva Kumar Review on the design modifications of a solar air heater for improvement in the thermal performance. Sustainable Energy Technologies and Assessments 39 (2020) 100685.

[34] Prasad BN, Saini JS. Optimal thermohydraulic performance of artificially roughened solar air heaters. Solar Energy 1991; 47:91–6.

[35] Prasad BN, Saini JS. Effect of artificial roughness on heat transfer and friction factor in a solar air heater. Solar Energy 1988; 41:555–60.

[36] Dengjia Wanga,⁎, Jin Liua, Yanfeng Liua, Yingying Wanga, Bojia Lib, Jiaping Liua, Evaluation of the performance of an improved solar air heater with "S" shaped ribs with gap, Solar Energy 195 (2020) 89–101.